Northumbria Research Link

Northumbria University NEWCASTLE

UniversityLibrary

Wind Power Prediction based on High-frequency SCADA data along with Isolation Forest and Deep Learning Neural Networks

Zi Lin[1], Xiaolei Liu[2*], Maurizio Collu[1]

[1]*Department of Naval Architecture, Ocean and Marine Engineering, University of Strathclyde, Glasgow, G4 0LZ, United Kingdom*
[2]*James Watt School of Engineering, University of Glasgow, Glasgow, G12 8QQ, United Kingdom*

Abstract

Wind power plays a key role in reducing global carbon emission. The power curve provided by wind turbine manufacturers offers an effective way of presenting the global performance of wind turbines. However, due to the complicated dynamics nature of offshore wind turbines, and the harsh environment in which they are operating, wind power forecasting is challenging, but at the same time vital to enable condition monitoring (CM). Wind turbine power prediction, using supervisory control and data acquisition (SCADA) data, may not lead to the optimum control strategy as sensors may generate non-calibrated data due to degradation. To mitigate the adverse effects of outliers from SCADA data on wind power forecasting, this paper proposed a novel approach to perform power prediction using high-frequency SCADA data, based on isolate forest (IF) and deep learning neural networks. In the predictive model, wind speed, nacelle orientation, yaw error, blade pitch angle, and ambient temperature were considered as input features, while wind power is evaluated as the output feature. The deep learning model has been trained, tested, and validated against SCADA measurements. Compared against the conventional predictive model used for outlier detection, i.e. based on Gaussian processes, the proposed integrated approach, which coupled IF and deep learning, is expected to be a more efficient tool for anomaly detection in wind power prediction.

Keywords Wind power prediction; Deep learning neural networks; Isolation forest; Outlier detection; Offshore wind turbines

Abbreviations

AI	Artificial Intelligence
ANN	Artificial Neural Networks
CFD	Computational Fluid Dynamics
CM	Condition Monitoring
EE	Elliptic Envelope
GP	Gaussian Process

---

* Corresponding author, E-mail: Xiaolei.Liu@glasgow.ac.uk (XL)

34	IEC	International Electrotechnical Commission
35	IF	Isolation Forest
36	NWP	Numerical Weather Prediction
37	ORE Catapult	Offshore Renewable Energy Catapult
38	O&M	Operations and Maintenance
39	PCA	Principal Component Analysis
40	PMG	Permanent Magnet Generator
41	ReLU	Rectified Linear Unit
42	RMSE	Root Mean Square Error
43	SCADA	Supervisory Control and Data Acquisition
44	SVMs	Support Vector Machines
45	SVR	Support Vector Regression

46

1.   Introduction

48   Wind power is well-thought-out as a promising source for electric generation, especially in terms of minimizing carbon

49 emission. Worldwide, the wind industry has seen a speedy growth of its business in the past few decades. For example, gross

50 installations of EU onshore and offshore wind were 0.3 GW in 2008, amplified to 3.2 GW in 2017 [1]. More specifically, in

51 2018, Germany, Spain, and the UK are the top three EU countries in terms of owning the largest cumulative capacities [1].

52 Moreover, in Denmark, more than 40% of annual electricity was generated by wind in the same year [1]. With the continuous

53 progress of wind turbine equipment, the rate of wind turbine installation has seen an increase. Benefited by the evolving

54 technology, progressively more new installed wind farms have moved from onshore to offshore. For instance, annual EU

55 installed offshore wind farms accounted for 12% of total installations in 2013, increased to 23.07% in 2018 [1]. Compared with

56 the onshore wind turbine, offshore wind turbines have a couple of key advantages, for example, a much lower level of noise

57 and a larger power output. On the other hand, different sources of challenges between onshore and offshore wind turbines, such

58 as a harsher environment and a complex, multidisciplinary dynamics of the system, have increased the challenge for the CM

59 of offshore wind farms, and hence more likely, resulting in a surge in Operations and Maintenance (O&M) costs.

60   Wind power forecasting is essential to wind farm CM. Theoretically, wind power can be evaluated by the following

61 equation [2]:

$$P = \frac{1}{2}\rho\pi R^2 C_P u^3 \tag{1}$$

62   Where P is the wind power, ρ and R are the air density and the rotor radius, respectively, u is the wind speed, and C_P is

63 the power coefficient, denoting power captured by the turbine in percentage.

64   **Eq. (1)** shows a theoretical estimation of wind turbine power. Usually, a smooth power curve, showing the relationship

65   between wind turbine powers and hub height wind speeds, is provided by wind turbine manufacturers [2]. Each wind turbine

66   has a unique power curve, showing the overall performance of the wind turbine, even when the detailed components of the

67   wind turbine generating system is unavailable [2]. However, due to the stochastic nature of the wind, and the non-linear,

68   multidisciplinary dynamics of offshore wind turbine systems, real wind turbine power outputs are scattered. The generated

69   power is discontinuous in nature and crucial to the stability of the power system [3]. Moreover, there is usually a multipart

70   nonlinear relationship among wind turbine components, making the physics-based models inferior to the data-driven models

71   [4]. Compared with physical models, non-parametric methods, for instance artificial neural networks (ANN) [2], have the

72   advantage of high reliability and low prediction errors [4]. In terms of O&M, wind turbine power output is an essential

73   parameter to be monitored. Precise power predicting is indispensable to wind turbine operators, as inaccuracies may result in

74   financial losses [5]. Yan and Ouyang [6] proposed a two-step modelling methodology for wind power prediction. The two

75   modelling processes include a tendency of wind power progress and a data-driven correction model. Through a comparison

76   between the traditional statistical model and the primary physical model, predictive accuracies can be improved up to 80%.

77   Castellani, et al [5] claimed that, in complex terrain, global performance based on ANN, hybrid ANN and computational fluid

78   dynamics (CFD) methods showed negligible differences, while local performance has seen a discrepancy.

79   In recent years, wind power forecasting based on data-mining approaches, which is a non-parametric method, is becoming

80   progressively popular. This is probably due to the fact that wind turbines rely on SCADA systems for control and performance

81   monitoring [7], and the system has an advantage in delivering power outputs by default, without additional costs [8]. Many

82   researchers have developed various methodologies for power prediction based on SCADA data. Fang et al. [9] applied wind

83   turbine meteorological and SCADA data, together with a Support Vector Regression (SVR) model, to build a wind power

84   predictive model. Correlation study showed that there is a relationship between the turbine active power and operational

85   conditions. Jabbari Ghadi [10] developed a hybrid method by using a SCADA database, showing that ANN plus Numerical

86   Weather Prediction (NWP) could increase the accuracy in short-term and extremely short-term power predictions.

87   Morshedizadeh et al. [4] performed correlation analyses on a number of signals from SCADA data, concluding that the

88   dynamics networks, which were built by the rotor speed, gear temperature, blade pitch angle and wind speed, have seen an

89   error reduction of 40%, compared with the networks relied on wind speed only.

90   However, special cautions must be paid when using SCADA data to monitor power outputs, due to the degradation of the

91   sensors [8]. To this end, some previous studies have focused on pre-processing SCADA's outliers. For example, Yang [11]

92   applied an algorithm based on individual SCADA data for pre-processing, to increase CM reliability, unlike the International

93   Electrotechnical Commission (IEC) standard. Besides, Manobel et al. [12] applied Gaussian Process (GP) filtering for SCADA

94   data pre-processing. An improvement of 25% Root Mean Square Error (RMSE) was achieved in terms of power forecasting

95   by their model, comparing with the standard method [12]. Wang et al. [13] proposed a probabilistic method to detect and reject

96   outliers, showing the advantage of dealing with the non-linear multivariate relationship among parameters, while retaining the

97   key statistical values of the power curve.

98   Nowadays, it is worth noting that power curve outlier rejections are still challenging and an active area of research[13].

99   Traditional outlier detection and removal technologies largely rely on the level experience of the engineers, leading to potential

100   uncertainties in power predictions. To solve this problem, the main, novel contribution of this paper is the application of IF in

101   outlier detection and elimination, which has not been applied before for wind turbine power prediction. Compared with the

102   commonly used outlier detection method based on Gaussian processes, the proposed method improves the accuracy in power

103   predictions.

104   The remainder of this paper is organized as follows: Section 2 discussed the features of the SCADA datasets used in this

105   study, obtained from a one-year high-frequency monitoring offshore wind turbine with a rated power of 7MW. Section 3

106   focused on a detailed description of IF and EE, including the methodology adopted to perform data outlier detection and

107   removal. Based on the outlier removal process presented in section 3, a deep learning neural networks configuration was

108   introduced in section 4. After that, power prediction results trained by datasets of raw SCADA, datasets after IF filtering, and

109   datasets after EE filtering were carried out and compared against each other in section 5, respectively. To conclude, a summary

110   of the key contributions of the present paper is given in section 6.

111   **2.   Turbine characteristics and SCADA data description**

112   **2.1. Definition of the 7MW wind turbine**

113   The target wind turbine is a 7MW demonstration offshore wind turbine locates at Levenmouth, Fife, Scotland, UK. It is a

114   three-bladed upwind wind turbine mounted on a jacket support structure. **Fig. 1** shows the configuration of the wind turbine

115   with a rotor diameter and a hub height of 171.2 m and 110.6 m, respectively. The total height of the turbine is 196 m, ranging

116   from blade tip to sea level. Regarding the operation regions, the designed cut-in, rated and cut-out speeds are 3.5, 10.5 and 25

117   m/s, respectively. As for the drivetrain system, a medium speed (400 rpm) is selected, connecting to a Permanent Magnet

118   Generator (PMG) and a full-power converter. Further specifications of the wind turbine are displayed in **Table 1**.
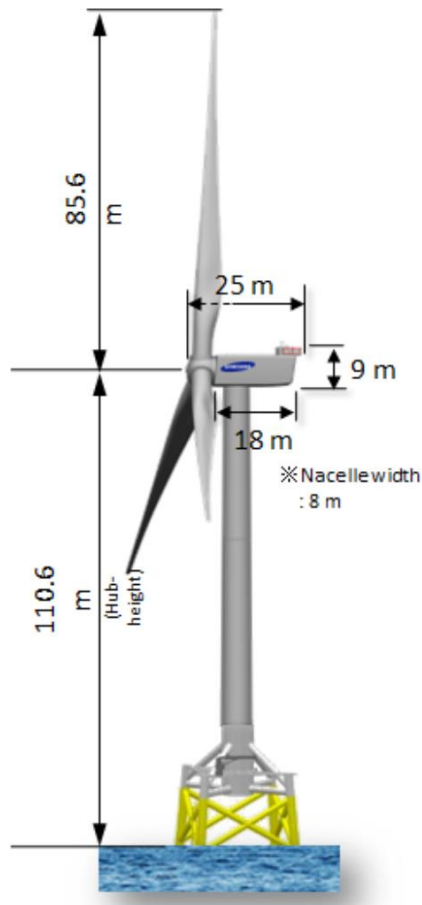
Fig. 1 – Layout the Levenmouth wind turbine [14].

Table 1 – Main properties of the 7MW wind turbine [14].

Properties	Value
Wind class	IEC class 1A
Rotor diameter	171.2m
Capacity	7 MW
Hub height	110.6m
Blade length	83.5m
Generator	Medium (3.3kV), PMG
Converter	Full power conversion
Drivetrain	400rpm
Rated frequency	50Hz
Rotor speed	5.9-10.6rpm
Wind speed	3.5-25m/s
Rated wind speed	10.9m/s
Design life	25years
Certification	DNV

2.2. SCADA data description and obvious error eliminating

The investigated SCADA datasets were recorded in the target offshore wind turbine for a one-year period from July 2018 to June 2019. These high-frequency data were provided in 1-second intervals. The offshore wind turbine is owned by the Offshore Renewable Energy (ORE) Catapult. In our deep learning neural networks, the investigated features were wind speed, wind direction, blade pitch angle, ambient temperature, and active wind power. As well known, wind direction can be derived from the position of the nacelle and yaw error. Therefore, in the current study, wind direction was represented by both nacelle orientation and yaw error. In total, there are five input features (wind speed, nacelle orientation, yaw error, blade pitch angle, and ambient temperature) and one output feature (generated wind power). The histograms of the raw SCADA datasets are presented in **Fig.2**.
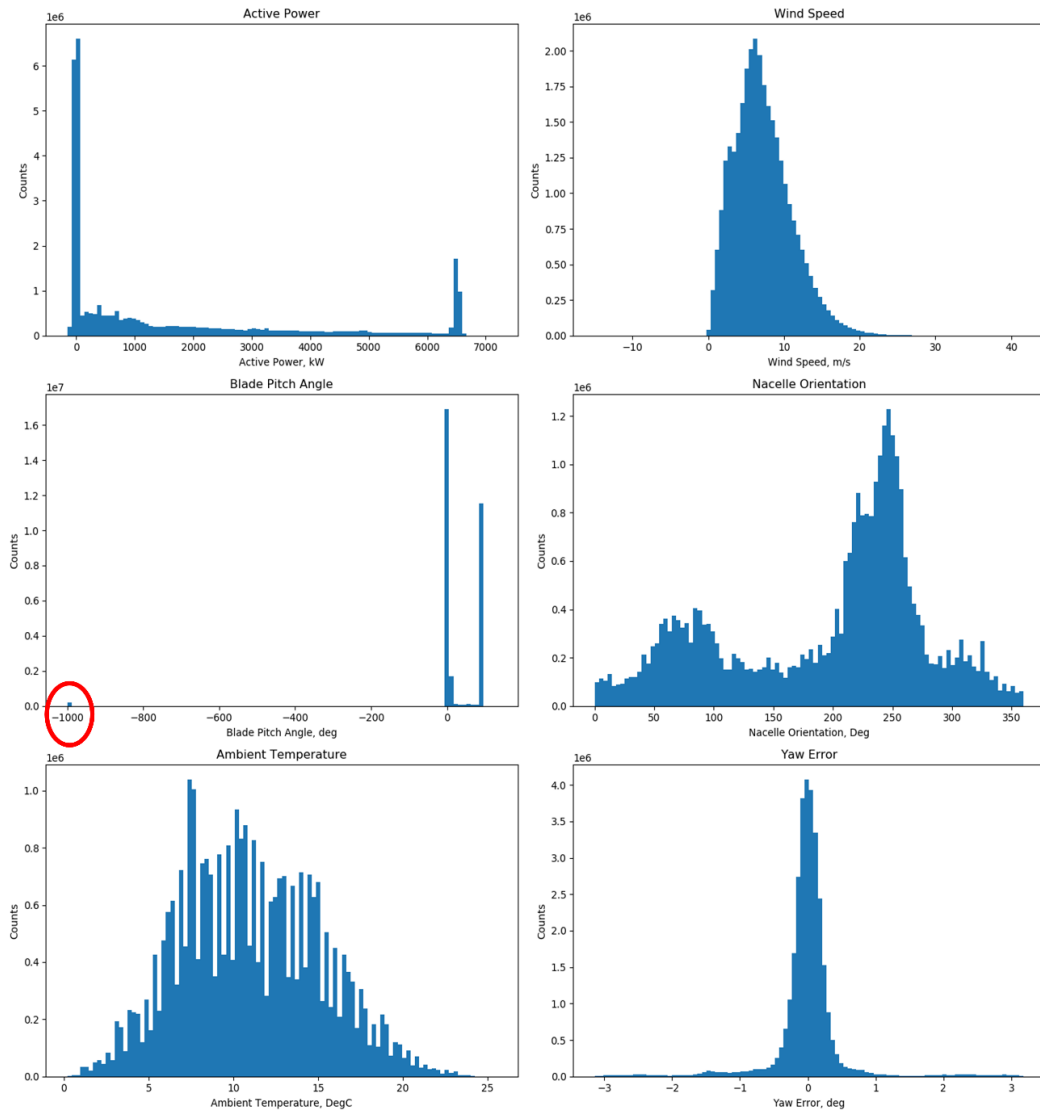

Fig. 2 – Histograms of selected input and output features in the raw SCADA datasets.

136   It can be seen that there are some obvious outliers (such as negative values) in the datasets of active power, wind speed,

137   and blade pitch angle. For instance, there is an outlier with a value of -1000° located at the left end of the histogram of blade

138   pitch angle (red circle in **Fig. 2**). Even if it is physically possible, there is no practical meaning for negative blade pitch angles.

139   The same theory can be generalized to negative wind speeds and negative powers. In this study, these obvious outliers were

140   automatically removed along with other corresponding parameters under the same time series. The updated histograms of

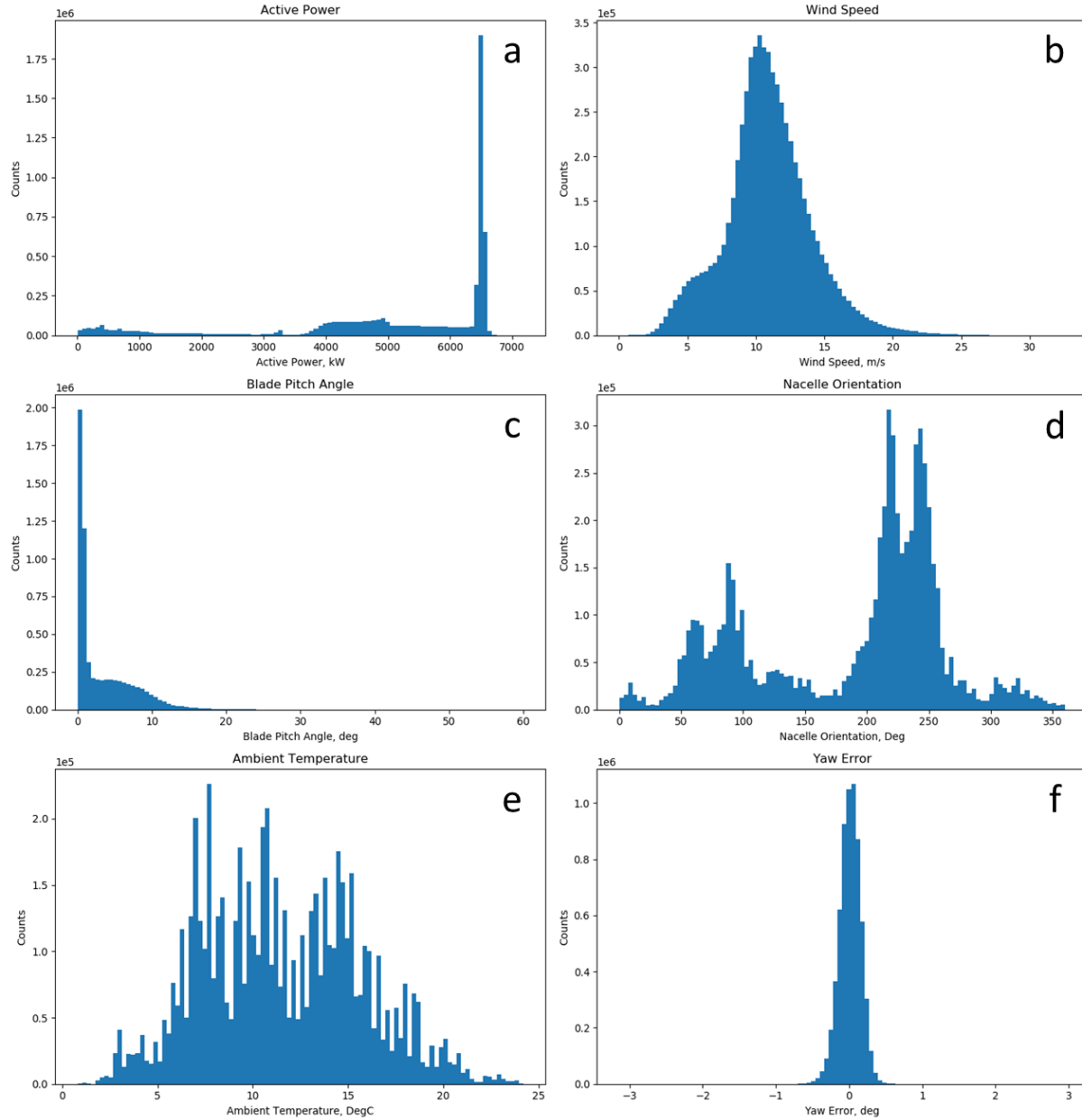141   selected input and output features are presented in **Fig.3**.

142

143   **Fig. 3** – Updated histograms of selected input and output features after obvious outlier detections.

144   The statistical details of percentile, count, mean, and standard deviation of the selected database were displayed in **Table**

145   **2**. The mean and median of wind speed were 10.9 and 10.7 m/s, respectively, which are similar to the rated wind speed of this

146   offshore wind turbine (10.9 m/s), indicating the generated active power is nearing the rated power (7 MW) in most of the

147   operating time (see **Fig. 3a**). For the same reason, the blade pitch angle variations were focused on the range of 3 ~ 4 deg (see

148   **Fig. 3c**). The mean of blade pitch angle is around 3.36 deg (see **Table 2**). The scatterings of wind speed, ambient temperature,

149   and yaw error obeyed normal distributions (see **Fig.3b, e,** and **f**). The scattering of nacelle orientation follows a bimodal

150   distribution (**Fig. 3d**), indicating the local wind can be roughly divided into two different directions.

151   **Table 2** – Statistical descriptions of the SCADA datasets.

	Active power, kW	Wind speed, m/s	Blade pitch angle, °	Nacelle orientation, °	Ambient temperature, °C	Yaw error, °
Count	6.33E+06	6.33E+06	6.33E+06	6.33E+06	6.33E+06	6.33E+06
Mean	5.13E+03	1.09E+01	3.36E+00	1.88E+02	1.15E+01	1.26E-02
Standard deviation	1.86E+03	3.18E+00	4.03E+00	7.74E+01	4.14E+00	1.45E-01
Minimum	1.00E+00	1.83E-02	1.54E-06	1.97E-03	8.00E-01	-3.14E+00
25%	4.41E+03	9.10E+00	3.47E-01	1.07E+02	8.10E+00	-7.84E-02
Median	6.02E+03	1.07E+01	1.19E+00	2.18E+02	1.11E+01	1.83E-02
75%	6.50E+03	1.27E+01	5.56E+00	2.42E+02	1.45E+01	1.10E-01
Maximum	7.18E+03	3.26E+01	6.00E+01	3.60E+02	2.42E+01	2.95E+00

152

3. Outlier detection

154   In data science, outliers are extreme values that deviate from normal observations within a database. In our SCADA

155   datasets, they represented a measuring variability, errors, or a novelty. In this study, the method of IF is used to detect data

156   points that diverge from the overall pattern on wind power prediction, which was further compared with the widely used outlier

157   detection method based on Gaussian processes.

3.1. Elliptic envelope

159   One of the widely accepted methods of performing outlier detection is to assume that the target datasets obeyed Gaussian

160   distribution, indicating the whole database is normally distributed. Under this assumption, the "shape" of the database is pre-

161   defined, where the observations that stand far away from the fitting shape would be detected as outliers. In this paper, the

162   Elliptic Envelope (EE) method was used and compared with IF in outlier detection by assuming our database is an expression

163   of a multivariate Gaussian distribution. It fits datasets into an ellipse to certain central data and recognized points outside the

164   central as outliers.

3.2. Isolation forest

166   The principle of IF is different from most other popular outlier detection methods (such as Gaussian processes), which

167   explicitly recognises anomalies instead of profiling normal datasets. Theoretically, normal data points occur more frequently

168   than outliers. Also, regular and abnormal observations are different from each other in terms of values. In most cases, outliers

169   are located further away from the regular data points in one feature space. Base on this fact, an abnormal point (see **Fig. 4b**)

170   requires fewer partitions to be identified than a normal one (see **Fig. 4a**). As the name of "Isolation Forest" indicates, this

171   algorithm is a type of tree ensemble methods that are based on decision trees. In a built IF, separations are firstly shaped by

172   randomly picking a feature and then selecting a random split value between the minimum and the maximum within the selected

173   feature [15].

174   Like other outlier detection techniques, IF uses anomaly scores for decision making. The anomaly score s of an instance

175   x can be defined as:

$$s(x,n) = 2^{-\frac{E(h(x))}{c(n)}} \tag{2}$$

176   where $h(x)$ is the path length of the point x; $E(h(x))$ is the average of $h(x)$ from a collection of isolation trees; $c(n)$ is

177   the average path length of unsuccessful search in a Binary Search Tree; n is the number of external nodes.

178   In this study, the anomaly score s returns 1 for normal data points and -1 for outliers.

179
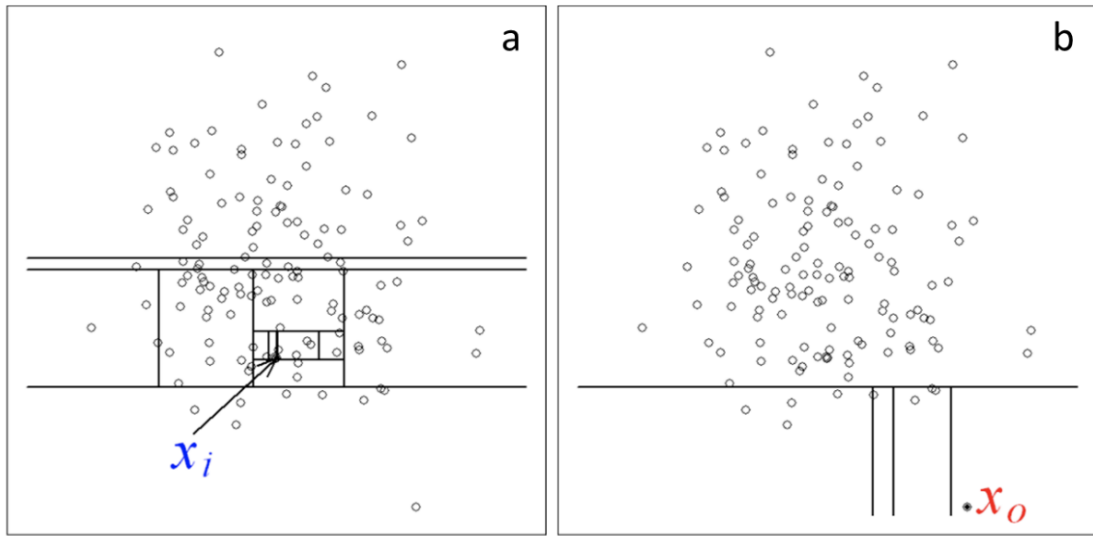
180   **Fig. 4** – Outliers (x_o) are more susceptible to isolation that normal observations (x_i), which have short path lengths [15].

181   **4. Deep Learning Neural Networks**

182   In this study, TensorFlow was used to develop a deep learning structure for wind power prediction, where the input tensor

183   was passed into the neural network and then output as another tensor (see **Fig. 5**). For getting better accuracy in predictions,

9

184   several network configurations were assessed, including changing of layers or node numbers in each trial. Consequently, a five-

185   layer deep learning neural network was selected to build the relationship between the inputs (see **Fig. 5A**) and the output (see

186   **Fig. 5G**). The deep learning model was trained by presenting it selected inputs (wind speed, nacelle orientation, yaw error,

187   blade pitch angle, and ambient temperature) and desired outputs (active power). Before tensors flowing into the designed

188   configuration, a Min-Max scaler is applied to scale training, testing, and validation data into the range of 0 ~ 1. The

189   corresponding formulation can be stated as:

$$X_{scaled} = \frac{x_i - \min{(x)}}{\max(x) - \min{(x)}} \tag{3}$$

190   where x_i is the original value; X_{scaled} is the normalized value; $\min{(x)}$ is the minimum value in the span; $\max(x)$ is the

191   maximum value in the span.

192   In the five-layer deep learning configuration, the first layer has 20 neurons (see **Fig. 5B**), while the second/third/fourth

193   layer has 50 neurons (see **Fig. 5C ~ E**), and the fifth layer has 20 neurons again (see **Fig. 5F**). As all the five layers shared a

194   similar internal structure, only layer 1 is extended and visualized in **Fig. 5B**. Each fully connected layer of the neural network

195   has three components:

196   ▪ A weight (w_{ij}) for each connection between each neuron and the neurons in the previous layer; in our deep learning

197   model, the algorithm of Xavier was selected to be used for weights initialization (see **Fig. 5B**);

198   ▪ A bias (b_j) for each neuron; the bias initialization was realized through the TensorFlow's built-in initializer function,

199   where the initial bias values of each neuron defaults as zero (see **Fig. 5B**);

200   ▪ An activation function ($ReLU(H_i)$) that outputs the result of the layer; the Rectified Linear Unit (ReLU) non-linear

201   activation function was selected in the current deep learning configuration (see **Fig. 5B**).

202   In summary, the following correlations are used to implement the fully connected layers:

$$H_i = \sum_{j=1}^{m} x_i w_{ij} + b_j \tag{4}$$

203   where H_i is the net input of neuron j in the output or deeper hidden layer; x_i is the input of neuron j; w_{ij} is the weights that

204   linked neuron i and j; b_j is the bias associated with neuron j.

$$h = ReLU(H_i) = \max{(0, H_i)} \tag{5}$$

205   where h is the output of neuron j.
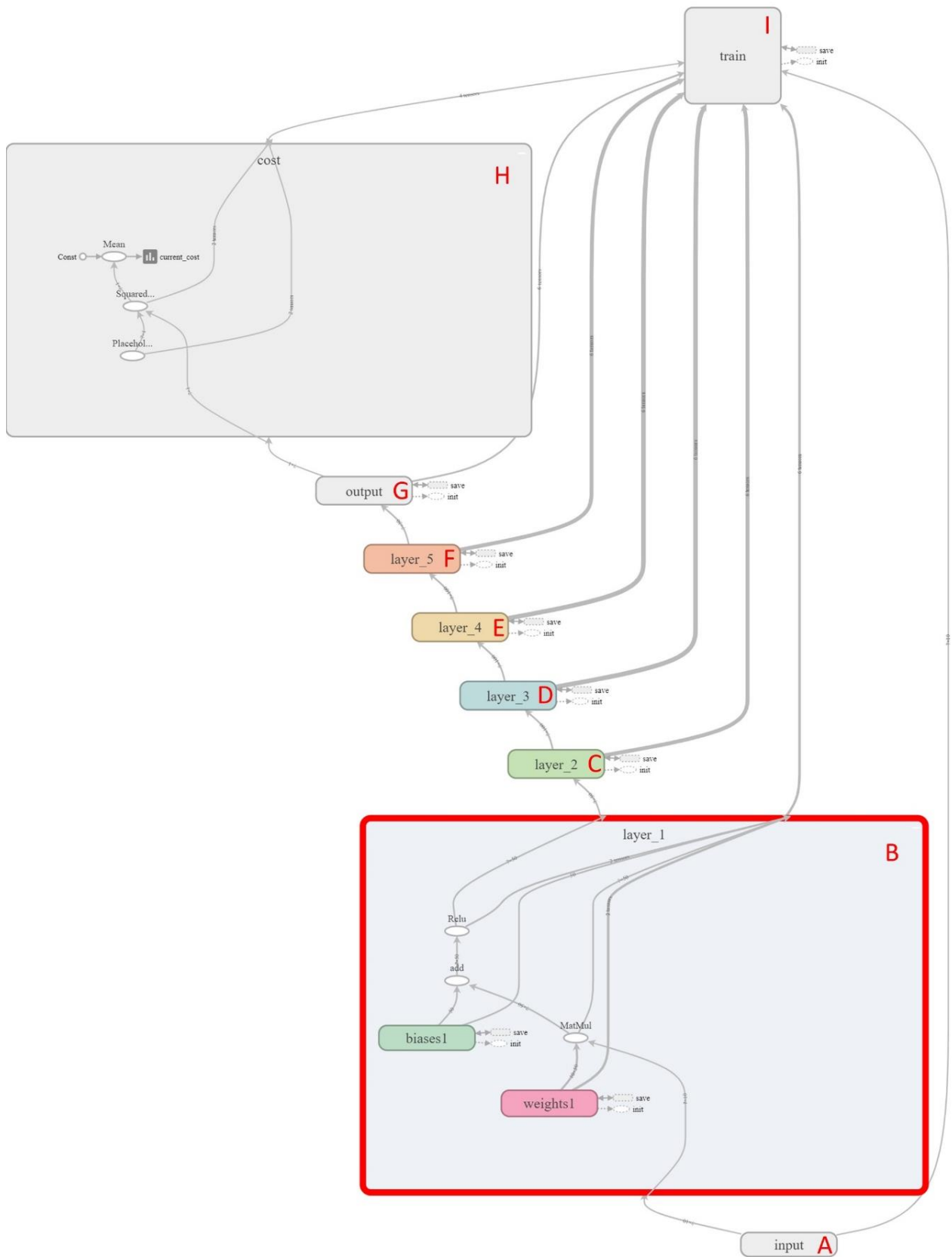
206

207   **Fig. 5** – Configuration of the designed deep learning neural networks.

208   In this study, the SCADA datasets were randomly divided into three groups – 70 % for training, 20% for testing, and 10%

209   for validation. While testing and validation datasets were kept as what they are, the raw SCADA training datasets were treated

210   by IF and EE, respectively. Therefore, three deep learning predictive models were built by training datasets of raw SCADA,

211   training datasets after IF filtering, and training datasets after EE filtering, respectively, following the classic train-test-validation

212   workflow. First, the training phase (see **Fig. 5I**) was carried out by presenting both training inputs and outputs to the neural

213   network while it learns how to transform input data to produce correct results. After the predictive model has been

214   trained, testing and validation datasets were fed into the model to make predictions. The loss function of Mean Square Error

215   (MSE) is used to resolve how far the predicted values deviate from the actual values in the testing/validation loops (see **Fig.**

216   **5H**), which can be expressed as:

$$MSE = \frac{1}{n}\sum_{i=1}^{n}\left[\frac{(M_{predicted})_i - (M_{actual})_i}{(M_{actual})_i}\right]^2 \tag{6}$$

217   where n is the number of tests; $(M_{predicted})_i$ is the predicted value of the ith tensor from the deep learning model;

218    $(M_{experimental})_i$ is the measured value of the ith tensor from the SCADA records.

219 **5.   Results and Discussions**

220 **5.1. Raw SCADA observations**

221   To investigate the influence of outlier detection on predictive results, the power curve of the selected wind turbine is

222   presented in **Fig.6**, using raw SCADA data from July 2018 to June 2019. SCADA measurements often contain erroneous data

223   caused by maintenance operations and breakdowns, which should not be used to perform wind power forecasting. There are

224   three types of operating issues can be obviously uncovered by viewing this power curve (corresponding to the two circles in

225   **Fig. 6**):

226   ▪   Constrained operation: several reasons can cause wind turbine performance to be artificially constrained. For

227   instance, a wind turbine should not generate any power that is higher than the rated power to avoid any potential

228   damage. In addition, the grid supply limitations require a curtailed power from time to time [16].

229   ▪   Over-measured wind speed: this issue can be caused by the inappropriate position of the anemometer [12], or the

230   natural degradation of sensors.

231   ▪   Turbine downtime: downtime could be identified from the power curve where wind speed is larger than the cut-

232   in speed but the generated power is null [17]. The detected downtimes could be further evaluated against operating

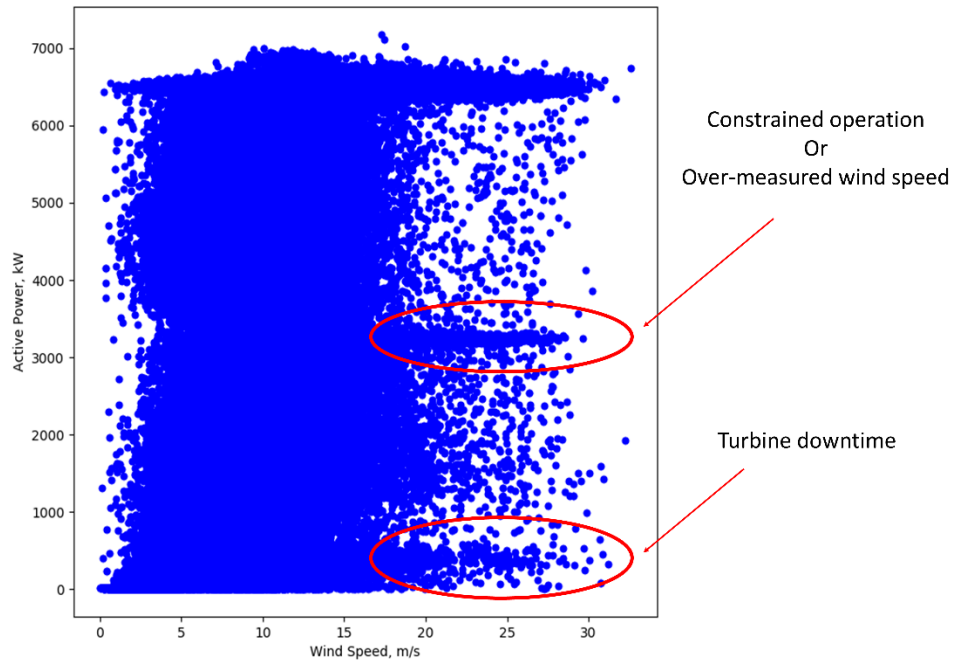233   logs to figure out unplanned downtimes.

234

235

236   **Fig. 6** – Raw wind turbine power curve with operating interference.

237   **5.2. Anomaly detection and treatment**

238   Both IF and EE are used for detecting and removing anomalies from SCADA datasets. The outlier fraction is defined as

239   12%, which kept 88% of what is reflected as normal data in both cases. In **Fig. 7a** and **b**, the detected anomalies are represented

240   by dotted points and normal data are indicated via full lines, where most detected anomalies were located at the boundaries of

241   the pattern. **Fig. 7c** and **d** displayed the power curves after IF and EE filtering, respectively, at which the detected outliers have

242   been discarded. As showed in **Fig. 7**, most of the outliers regarding breakdowns and maintenance operations have been cast-
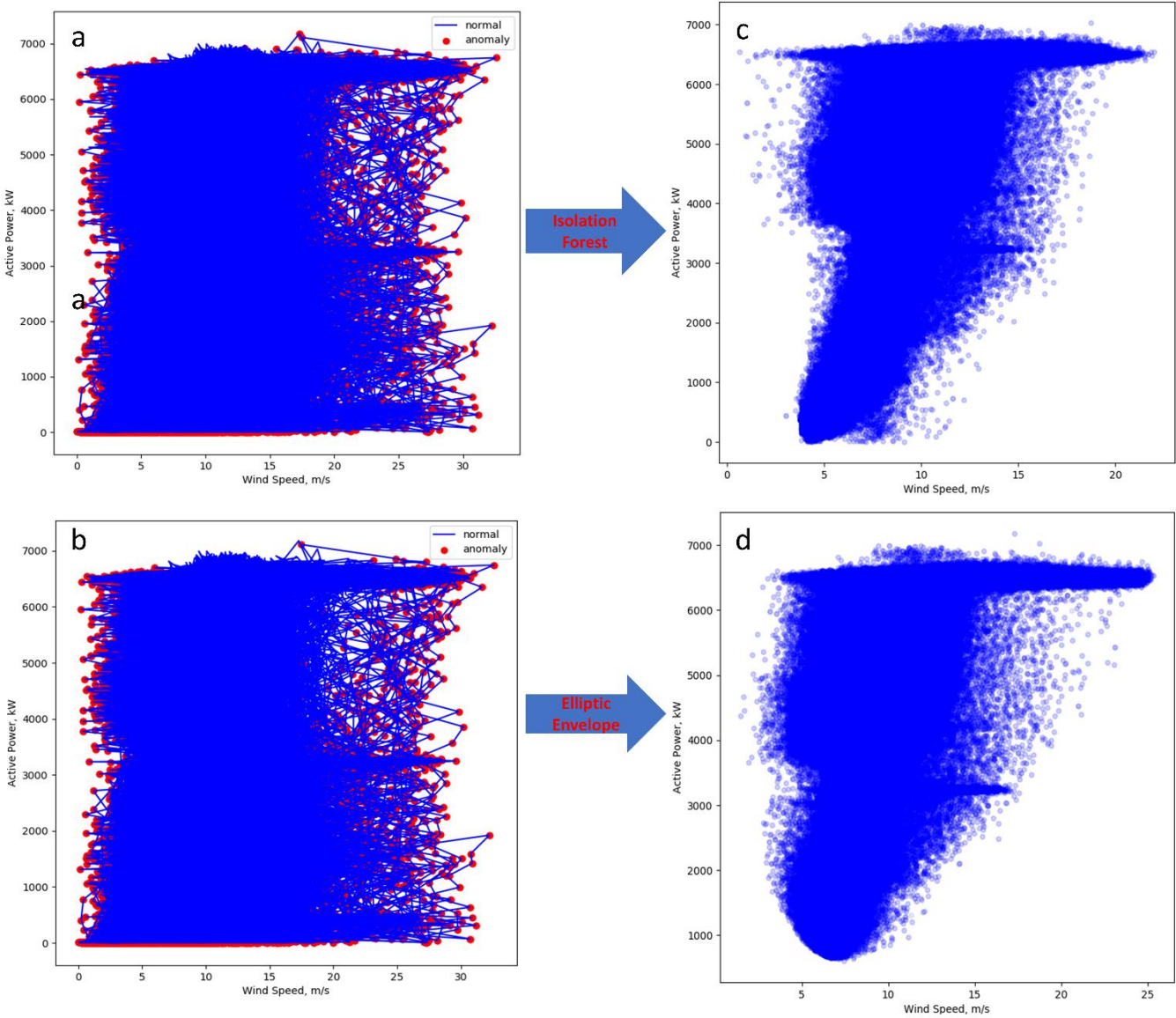
243   off.

244

245

Fig. 7 – Anomaly detection (a & b) and remove (c & d) via IF and EE in the one-year SCADA datasets.

5.3. Accuracy of forecasting

While the deep learning configuration was kept as it is, the training database was altered at each trial to investigate the impact of different outlier detection algorithms on predictive models by using training datasets of raw SCADA, training datasets after IF filtering, and training datasets after EE filtering, respectively. Then, the three predictive models were further examined through identical testing/validation datasets. Comparisons of MSE profiles in validation loops was presented in **Fig. 8**, where the distinguish among the three curves were obvious. For the deep learning predictive model without outlier filtering, it fails to converge after 200 epochs. On the other hand, for the cases with IF and EE filtering, the predictive model started to converge after around 100 epochs. The MSE profiles were initially decreasing during the transient period and then became flat as soon as the neural networks turned out to be stable. After detecting and removing extreme points in the used database, the deep

256 learning model can be trained more accurately and more smoothly. As presented in the zoom-in session of the last parts of MSE

257 profiles in **Fig. 8**, comparing with EE filtering, IF filtering provided a more accurate prediction with lower error values. The

258 network model was stabilized while MSEs equal to 0.003 and 0.004 for IF filtering and EE filtering, respectively. Even both

259 of outlier detection methods showed a similar trend, the accuracy of deep learning has been boosted when IF was used.
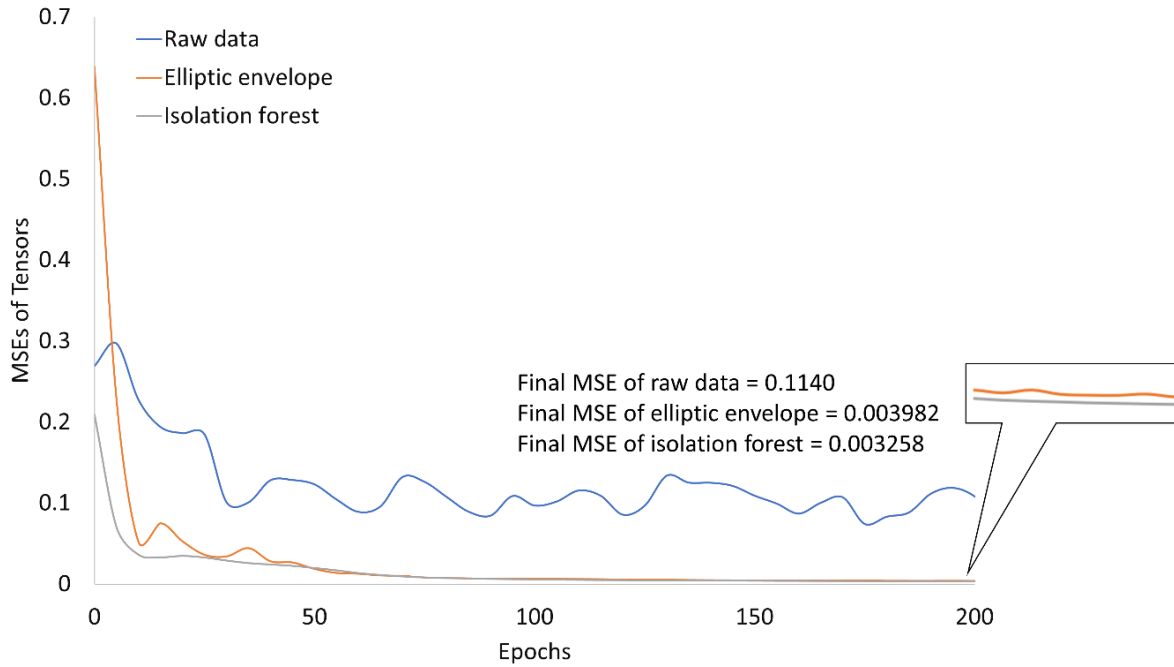
260

261 **Fig. 8 –** Variations of testing MSEs along 200 epochs with predictive models trained by raw data, database filtered by IF, and
262 database filtered by EE in an identical deep learning configuration.

263   The active power that was forecasted by the three deep learning predictive models is compared with the actual SCADA

264 measurements in **Fig. 9**. The worst scenario was observed in the case of raw SCADA data (**Fig. 9a**), indicating the deep learning

265 neural network has become an arbitrarily predictive model without outlier filtering. The predictive model with EE filtering

266 (**Fig. 9b**) performed better than the case of raw SCADA data. However, when wind speeds are in the range of 15 ~ 25 m/s,

267 predictive results obviously overestimated active powers. The best forecasting results were achieved by the case with IF (**Fig.**

268 **9c**), where a good agreement was achieved under most data points.

Deep learning trained by datasets of raw SCADA
Deep learning trained by datasets after EE filtering
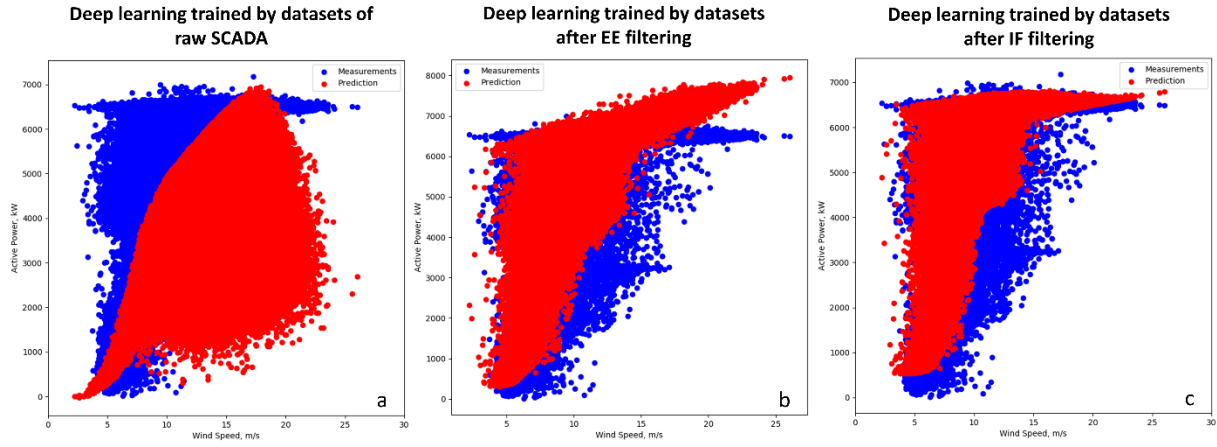**Deep learning trained by datasets after IF filtering**

Fig. 9 – Comparison of wind power curves between deep learning model (red dotted points) for raw SCADA data (a), IF (b), EE (c), and actual SCADA records (blue dotted points) respectively.

Based on the performance of the three predictive models in **Fig. 9**, it is confirmed that anomalies could not be appropriately identified by deep learning neural networks, and will give negative influences on their global performance. The reasons why IF offered better performance in wind power forecasting could be summarized as: EE is a very effective method if the considered datasets can be represented by the Gaussian distribution. This is why it is so widely used in outlier detection. However, it is not recommended to use EE when the datasets cannot be assumed to be modelled with a parametric method. In our SCADA database, the generated active power is not completely following a normal distribution, as its values are close to the rated power of 7 MW in most of the operating time (see **Fig. 3a**), triggered by the harsh offshore environment. On the other hand, IF can be considered as an effective method when Gaussian distributions cannot be assumed [18]. Furthermore, to capture the stochastic nature of the wind, the current study is using a very high-frequency SCADA database, with a sampling rate of 1 second, which created large-sized datasets with high dimensional input features, including wind speed, nacelle orientation, yaw error, blade pitch angle, and ambient temperature. Comparing with EE, IF can better handle large datasets with high dimensions [19].

6. Conclusions

This paper presented an integrated approach that coupled IF and deep learning for wind power prediction, based on input features of wind speed, nacelle orientation, yaw error, blade pitch angle, and ambient temperature. Compared with EE, the anomaly detection technique of IF further improved the global predictive performance of deep learning. Due to the advantages of the current coupled approach, this model is expected to be more effective in wind power forecasting from offshore wind turbines. Based on the facts above, this paper has the following conclusions:

- In this study, a deep learning neural network model was constructed to predict power for an offshore wind turbine in Scotland. Advanced data filtering techniques were applied to the inputs, before they were used for the training

292　　　phase of the network model. Deep learning predictive models can perform well only when they are trained with

293　　　filtered data. Using raw data would insert uncertainties in the predictive models.

294　　　▪ Even if the predictive models performed acceptably when adopting an EE filtering, pre-processing the data by IF

295　　　can improve the accuracy of the deep learning method. The anomalies that are related to constrained operations

296　　　and turbine downtime have been automatically detected and removed from the SCADA database. Deep learning

297　　　neural networks presented its full advantage while combined with IF.

298　　　▪ Due to the stochastic nature of the offshore wind, its speed and direction vary with a very small period (few

299　　　seconds or shorter), generating high-fluctuating, high-dimensional and large-sized SCADA database. Results

300　　　showed that, when compared with commonly used outlier detection method based on Gaussian processes, IF is a

301　　　more effective method, since it is more robust when the input features used in wind power prediction cannot be

302　　　assumed to be Gaussian.

303 **Acknowledgement**

305 **References**

306 [1] Komusanac I, Fraile D, Brindley G. Wind energy in Europe in 2018 - Trends and statistics. 2019.

307 [2] Lydia M, Kumar SS, Selvakumar AI, Prem Kumar GE. A comprehensive review on wind turbine power curve

308　　　modeling techniques. Renewable and Sustainable Energy Reviews 2014;30:452–60. doi:10.1016/j.rser.2013.10.030.

309 [3] Saleh AE, Moustafa MS, Abo-Al-Ez KM, Abdullah AA. A hybrid neuro-fuzzy power prediction system for wind

310　　　energy generation. International Journal of Electrical Power and Energy Systems 2016;74:384–95.

311　　　doi:10.1016/j.ijepes.2015.07.039.

312 [4] Morshedizadeh M, Kordestani M, Carriveau R, Ting DSK, Saif M. Improved power curve monitoring of wind

313　　　turbines. Wind Engineering 2017;41:260–71. doi:10.1177/0309524X17709730.

314 [5] Castellani F, Astolfi D, Mana M, Burlando M, Meißner C, Piccioni E. Wind Power Forecasting techniques in

315　　　complex terrain: ANN vs. ANN-CFD hybrid approach. Journal of Physics: Conference Series 2016;753.

316　　　doi:10.1088/1742-6596/753/8/082002.

317 [6] Yan J, Ouyang T. Advanced wind power prediction based on data-driven error correction. Energy Conversion and

318　　　Management 2019;180:302–11. doi:10.1016/j.enconman.2018.10.108.

319 [7] Burton T, Sharpe D, Jenkins N, Bossanyi E. Wind Energy Handbook. John Wiley & Sons; 2001.

320 [8] Ziegler L, Gonzalez E, Rubert T, Smolka U, Melero JJ. Lifetime extension of onshore wind turbines : A review

321 covering Germany ,. Renewable and Sustainable Energy Reviews 2018;82:1261–71. doi:10.1016/j.rser.2017.09.100.

322 [9] Fang R, Wang Y, Shang R, Liang Y, Wang L, Peng C. The ultra-short term power prediction of wind farm

323 considering operational condition of wind turbines. International Journal of Hydrogen Energy 2016;41:15733–9.

324 doi:10.1016/j.ijhydene.2016.03.173.

325 [10] Ghadi MJ, Gilani SH, Afrakhte H, Baghramian A. A novel heuristic method for wind farm power prediction: A case

326 study. International Journal of Electrical Power and Energy Systems 2014;63:962–70.

327 doi:10.1016/j.ijepes.2014.07.008.

328 [11] Yang W, Court R, Jiang J. Wind turbine condition monitoring by the approach of SCADA data analysis. Renewable

329 Energy 2013;53:365–76. doi:10.1016/j.renene.2012.11.030.

330 [12] Manobel B, Sehnke F, Lazzús JA, Salfate I, Felder M, Montecinos S. Wind turbine power curve modeling based on

331 Gaussian Processes and Artificial Neural Networks. Renewable Energy 2018;125:1015–20.

332 doi:10.1016/j.renene.2018.02.081.

333 [13] Wang Y, Infield D, Stephen B, Galloway S. Copula-based model for wind turbine power curve outlier rejection.

334 Wind Energy 2014;18:1875–91. doi:10.1002/we.

335 [14] Serret J, Rodriguez C, Tezdogan T, Stratford T, Thies P. Code comparison of a NREL-fast model of the levenmouth

336 wind turbine with the GH bladed commissioning results. Proceedings of the International Conference on Offshore

337 Mechanics and Arctic Engineering - OMAE, 2018. doi:10.1115/OMAE2018-77495.

338 [15] Liu FT, Ting KM, Zhou Z. Isolation Forest. Proceedings of the 2008 Eighth IEEE International Conference on Data

339 Mining. IEEE Computer Society, 2008, p. 413–22.

340 [16] Jiang Y, Guo L, You S. Research on nodal wind power values and optimal accommodation based on locational

341 marginal price. International Journal of Electrical Power and Energy Systems 2019;109:343–50.

342 doi:10.1016/j.ijepes.2019.02.001.

343 [17] Zhu Y, Zhu C, Song C, Li Y, Chen X, Yong B. Improvement of reliability and wind power generation based on wind

344 turbine real-time condition assessment. International Journal of Electrical Power and Energy Systems 2019;113:344–

345 54. doi:10.1016/j.ijepes.2019.05.027.

346 [18] Wang Y-B, Chang D-G, Qin S-R, Fan Y-H, Mu H-B, Zhang G-J. Separating Multi-Source Partial Discharge Signals

347 Using Linear Prediction Analysis and Isolation Forest Algorithm. IEEE Transactions on Instrumentation and

348 Measurement 2019;PP:1–1. doi:10.1109/tim.2019.2926688.

349   [19]   Puggini L, McLoone S. An enhanced variable selection and Isolation Forest based methodology for anomaly

350   detection with OES data. Engineering Applications of Artificial Intelligence 2018;67:126–35.

351   doi:10.1016/j.engappai.2017.09.021.

352